Energy partition on marine converted waves

Carlos A. Cunha Filho

ABSTRACT

A simple marine model, comprised of two elastic layers overlaid by water, is used to study the four principal reflection modes present in marine seismic reflection data. The energy distribution between the phases depends on the elastic and geometric parameters; this dependence is evaluated as a function of offset. It is shown that the critical angle for P waves on the first layer beneath the water, determines the lower offset limit for measurable converted waves. Beyond this limit, the offset dependence of PSSP amplitude was found not to be controlled by the conversion process, but instead by the subsurface properties.

INTRODUCTION

The use of relative shear wave and compressional wave velocities to determine lithologic properties has been studied by several authors (Domenico, 1984; Tatham, 1982). One way of indirectly obtaining this information from conventional seismic data is from amplitude analysis. Rosa (1976) and Ostrander (1984) studied the use of the PP reflection coefficient variation with offset as a direct gas indicator. For land data, both P and S waves can be (to some degree) generated and recorded independently, but the high cost of this technique has limited its routine application.

Marine data, however, has some intrinsic features that can be very useful for determination of P and S velocities. The medium in which the source and receiver are located is homogeneous and has known properties. Only P waves are generated and recorded, instead of an unknown superposition of P, SV and SH as happens in conventional land data. The possibility of processing converted waves in marine data has not yet been completely studied. Tatham and Stoffa (1976) used traveltime differences between marine PPPP and PSSP stacked sections as an indication of hydrocarbon presence. In this work, we used a simplified model to study the different factors that affect the energy partitioning among the recorded modes. The offset

range in which the energy in converted modes becomes comparable to pure P waves is determined for a particular case. We found that the offset beyond which the conversion process becomes relevant, is a function of the critical angle for P waves incident on the sea bottom (which depends on the first layer velocity). Another important result is that beyond the P-wave critical offset, the variation of PSSP amplitude with offset and the energy balance between PPPP and PSSP are dependent on the elastic parameters and can be used to supplement the conventional AVO (amplitude versus offset) methods.

A SIMPLIFIED MODEL

Figure 1 shows the basic model studied here: a water layer and two solid layers with density ρ, P wave velocity α, and Poisson's ratio σ. Only the waves associated with primary reflections on the interface between the second and third layers are considered.

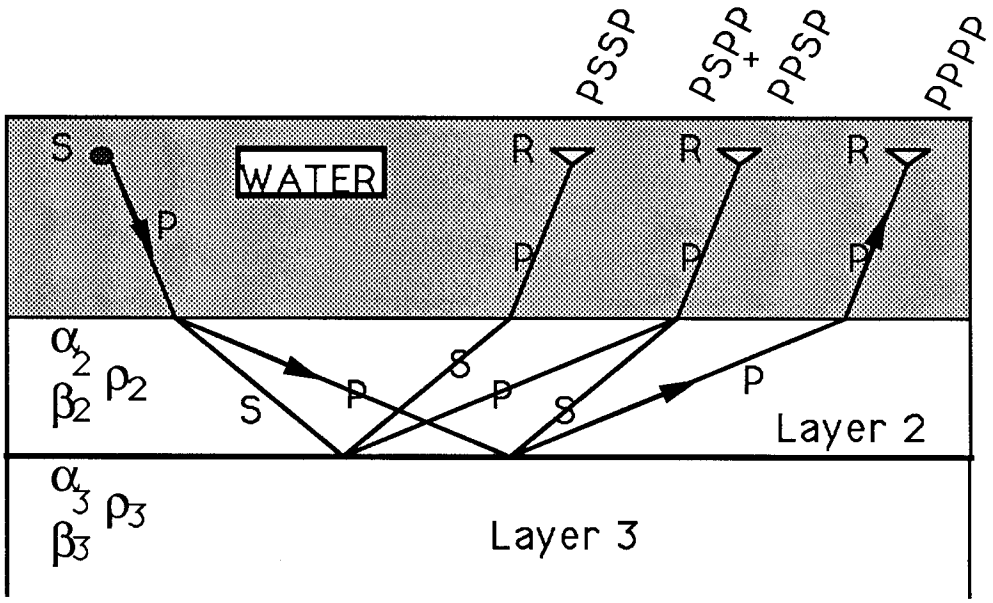

FIG. 1. converted waves in a three layer marine model

We can see that:

- There are two phase generations at the passage through the first interface and two more at the reflection on the second interface; these four correspond to the recorded waves PPPP, PPSP, PSPP and PSSP.
- When the layers are horizontal, PSPP and PPSP are recorded at the same offset at the same traveltime and so can be considered a single wave.

- Even though PSSP amplitude becomes relevant only at large angles, the horizontal slowness of the recorded PSSP is larger than that of the PPPP for a given receiver, because for a given angle of incidence, PSSP will be received at a lower offset than PPPP.

THE SCATTERING MATRIX

Following Aki-Richards (1980) conventions (Figure 2), we can represent the rela-

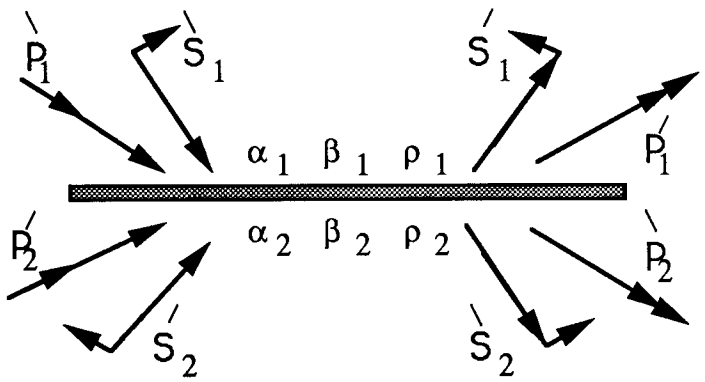

FIG. 2. Incident and scattered waves at an interface

tion between the amplitudes of the incident waves (lefthand side) and the amplitudes of the scattered waves (righthand side) by:

$$\begin{pmatrix} \acute{P}_1 \\ \acute{S}_1 \\ \grave{P}_2 \\ \grave{S}_2 \end{pmatrix} = \begin{pmatrix} \grave{P}\acute{P} & \grave{S}\acute{P} & \acute{P}\acute{P} & \acute{S}\acute{P} \\ \grave{P}\acute{S} & \grave{S}\acute{S} & \acute{P}\acute{S} & \acute{S}\acute{S} \\ \grave{P}\grave{P} & \grave{S}\grave{P} & \acute{P}\grave{P} & \acute{S}\grave{P} \\ \grave{P}\grave{S} & \grave{S}\grave{S} & \acute{P}\grave{S} & \acute{S}\grave{S} \end{pmatrix} \begin{pmatrix} \grave{P}_1 \\ \grave{S}_1 \\ \acute{P}_2 \\ \acute{S}_2 \end{pmatrix}$$

or

$$\mathbf{O} = S\mathbf{I}$$

where **I** is the amplitude vector of the incident field, **O** the amplitude vector of the scattered field, and S, the scattering matrix defined in terms of energy flux (Frasier, 1970), is an hermitian operator. The above relation can be put in a simpler form:

$$\begin{pmatrix} \acute{O}_i \\ \grave{O}_{i+1} \end{pmatrix} = \begin{pmatrix} \check{S} & \acute{S} \\ \grave{S} & \hat{S} \end{pmatrix} \begin{pmatrix} \grave{I}_i \\ \acute{I}_{i+1} \end{pmatrix}$$

It is important to mention that as the scattering matrix depends not only on the properties of the two media but also on the angles of the incident and scattered waves, all the components of **I** and **O** must have the same horizontal slowness p. This condition is satisfied by the model comprised of horizontal layers.

For the downgoing waves the propagation will be represented by

$$\grave{\mathbf{I}}_{\mathbf{i}} = \grave{\mathbf{O}}_{\mathbf{i}}$$

and the upcoming waves by

$$\acute{\mathbf{I}}_{\mathbf{i}} = \acute{\mathbf{O}}_{\mathbf{i}}$$

For convenience, we separated the scattered field into their P and S components:

$$\grave{\mathbf{O}}_{\mathbf{i}} = \begin{cases} \grave{\mathbf{I}}_{\mathbf{Pi}} = \begin{pmatrix} \grave{P}_i \\ 0 \end{pmatrix} \\ \\ \grave{\mathbf{I}}_{\mathbf{Si}} = \begin{pmatrix} 0 \\ \grave{S}_i \end{pmatrix} \end{cases} \qquad \acute{\mathbf{O}}_{\mathbf{i}} = \begin{cases} \acute{\mathbf{I}}_{\mathbf{Pi}} = \begin{pmatrix} \acute{P}_i \\ 0 \end{pmatrix} \\ \\ \acute{\mathbf{I}}_{\mathbf{Si}} = \begin{pmatrix} 0 \\ \acute{S}_i \end{pmatrix} \end{cases}$$

As we are interested only in the reflection from a particular interface (without multiples), only $\grave{\mathcal{S}}$ needs to be considered for the downgoing wave:

$$\grave{\mathbf{O}}_{\mathbf{i+1}} = \grave{\mathcal{S}}\ \grave{\mathbf{I}}_{\mathbf{i}}$$

At the reflector n, only $\check{\mathcal{S}}$ must be take into account:

$$\acute{\mathbf{O}}_{\mathbf{i}} = \check{\mathcal{S}}\ \grave{\mathbf{I}}_{\mathbf{i}}$$

And, for the upcoming waves,

$$\acute{\mathbf{O}}_{\mathbf{i}} = \acute{\mathcal{S}}\ \acute{\mathbf{I}}_{\mathbf{i+1}}$$

The number of different waves recorded is $3 \times 4^{n-1}$, where n is the number of layers traveled (other than water). In the present case ($n = 1$) there will be three distinct phases, whose recorded relative amplitudes are given by

$$\mathcal{A}_{PPPP} = \{(\grave{P}\grave{P})_{1-2}(\grave{P}\acute{P})_{2-3}(\acute{P}\acute{P})_{1-2}\}\mathcal{A}_I \tag{1}$$

$$\mathcal{A}_{PPSP+PSPP} = \{(\grave{P}\grave{P})_{1-2}(\grave{P}\acute{S})_{2-3}(\acute{S}\acute{P})_{1-2} + (\grave{P}\grave{S})_{1-2}(\grave{S}\acute{P})_{2-3}(\acute{P}\acute{P})_{1-2}\}\mathcal{A}_I \tag{2}$$

$$\mathcal{A}_{PSSP} = \{(\grave{P}\grave{S})_{1-2}(\grave{S}\acute{S})_{2-3}(\acute{S}\acute{P})_{1-2}\}\mathcal{A}_I \tag{3}$$

The relative amplitudes of these three phases are plotted on Figures 3, 4 and 5 as a function of the angle of incidence, for three different sets of elastic parameters. Although spherical-wave coefficients (Claerbout, 1984) should be used to study the near-field behavior, the use of plane-wave coefficients is a good approximation for the far field.

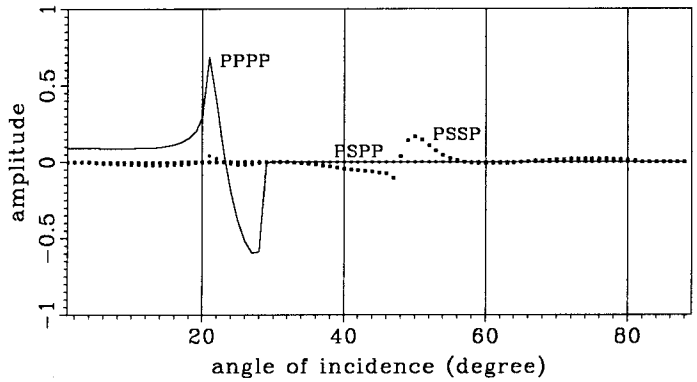

FIG. 3. Relative amplitude of the phases for $\alpha_2 = 3000$ m/s, $\alpha_3 = 4000$ m/s, $\sigma_2 = \sigma_3 = .33$ and $\rho_2 = \rho_3 = 2$ g/cc.

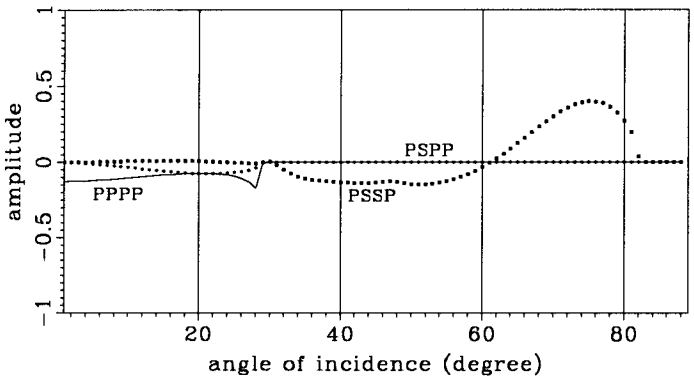

FIG. 4. Relative amplitude of the phases for $\alpha_2 = 3000$ m/s, $\alpha_3 = 2000$ m/s, $\sigma_2 = \sigma_3 = .33$ and $\rho_2 = \rho_3 = 2$ g/cc.

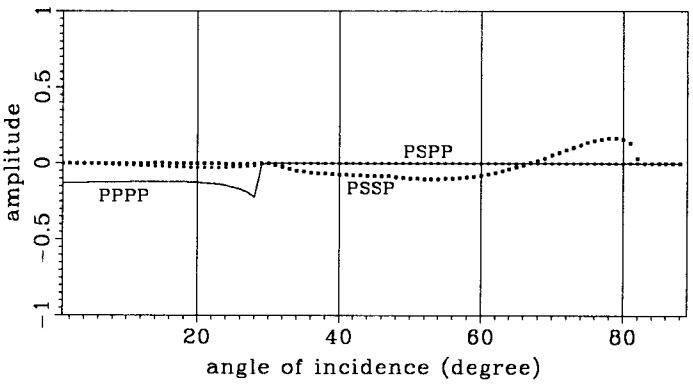

FIG. 5. Relative amplitude of the phases for $\alpha_2 = 3000$ m/s, $\alpha_3 = 2000$ m/s, $\sigma_2 = .33$, $\sigma_3 = .10$ and $\rho_2 = \rho_3 = 2$ g/cc.

WHEN IS CONVERSION RELEVANT?

The critical angle for P waves on the second layer is a sort of dividing line. Below this angle, PPPP and PSPP+PPSP are dominant, while above it only PSSP is present. In Figure 4 there is no contrast of the Poisson's ratio, while in Figure 5 the Poisson's ratio varies from .33 in the second layer to .10 in the next one; this variance simulates the presence of gas in the third layer (Domenico, 1984). As expected, the PPPP amplitude is larger and has a steeper increase with angle of incidence when gas is present, while both PSPP and PSSP show a uniform decrease of amplitude for all angles. The synthetic seismograms for the conditions represented in Figures 4 and 5 are shown in Figure 6.

To make a realistic evaluation of the relative amount of converted energy present on conventional marine seismic data, it is necessary to analyze the energy partition as a function of offset. In making this analysis, we have made use of a standard model, with the following characteristics:

- $\alpha_2 = 3000$ m/s and $\alpha_3 = 4000$ m/s
- $\sigma_2 = \sigma_3 = .33$ and $\rho_2 = \rho_3 = 2$ g/cc
- $z_1 = 250$ m and $z_2 = 2000$ m

where z_1 and z_2 are the depths of the first and second interfaces. Unless it is explicitly stated, the above parameters are implied.

To better understand the partitioning of energy among the different phases, we focus our attention on the PSSP mode and uncouple the two distinct processes involved on this simplified model: the conversion process (P into S and S into P), that takes place on the water-second layer interface, and the SS reflection on the second-third layer interface.

The PS (or SP) conversion coefficient is shown on Figure 7 as a function of the angle of incidence and P wave velocity of the second layer. There is a reasonable amount of conversion for almost all velocities and again we can see that the critical angle for P waves has a key role on the process. For high velocities the S wave critical angle also becomes relevant.

To analyze the behavior of the SS reflection coefficient we must to hold constant the velocity of one of the layers.

Figure 8 shows the dependence of the SS reflection on the third layer's P velocity and on the angle of incidence on the sea bottom (so that a direct comparison with Figure 7 is possible); the P velocity in the second layer was kept constant (3000 m/s).

The SS reflection coefficient is much more sensitive to changes of the velocities then is the conversion factor, and so the recorded PSSP wave will carry more information related to the subsurface lithology than to the first layer's composition. We

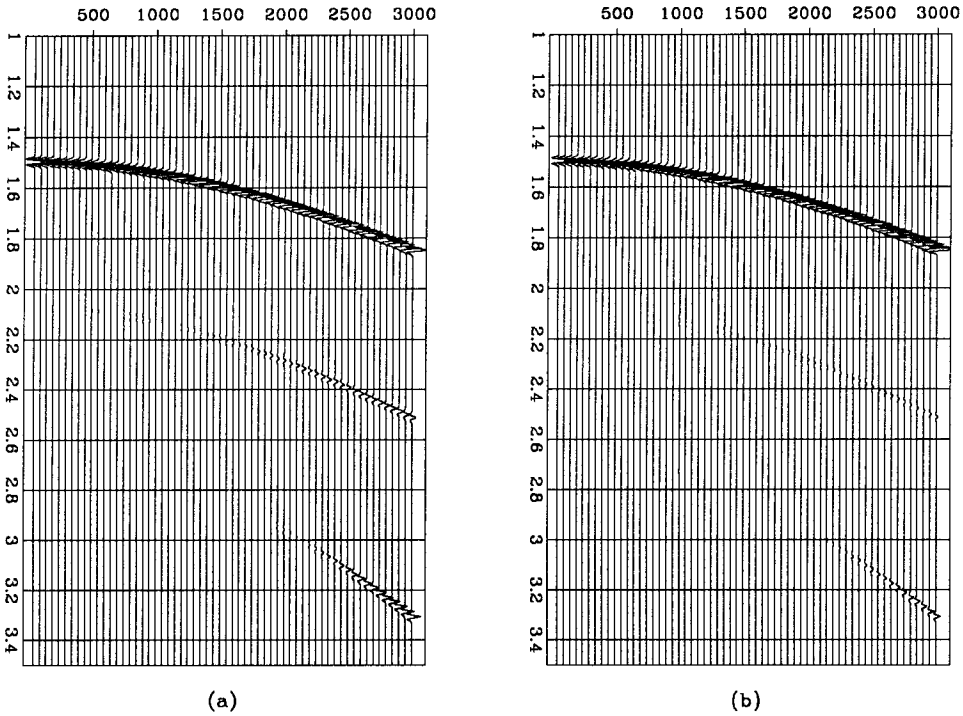

FIG. 6. Synthetic seismograms for the conditions shown in Figures 4 and 5: (a) no gas ($\sigma_3 = .33$) and (b) gas in third layer ($\sigma_3 = .10$).

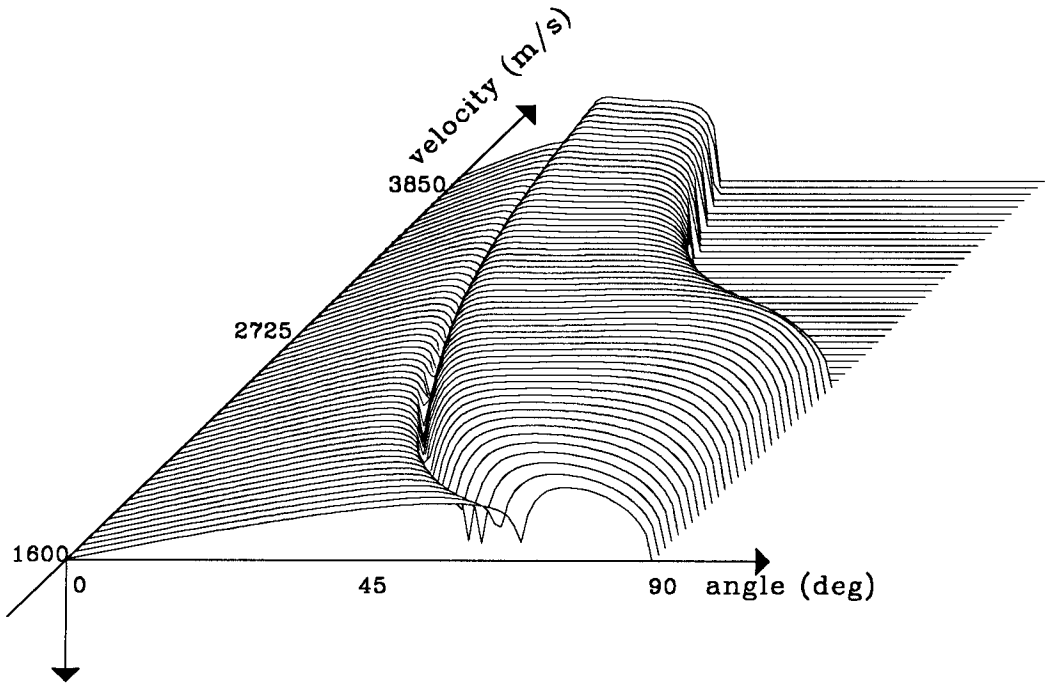

FIG. 7. PS conversion coefficient (negative values are plotted upward) as a function of α_2 and the angle of incidence on water.

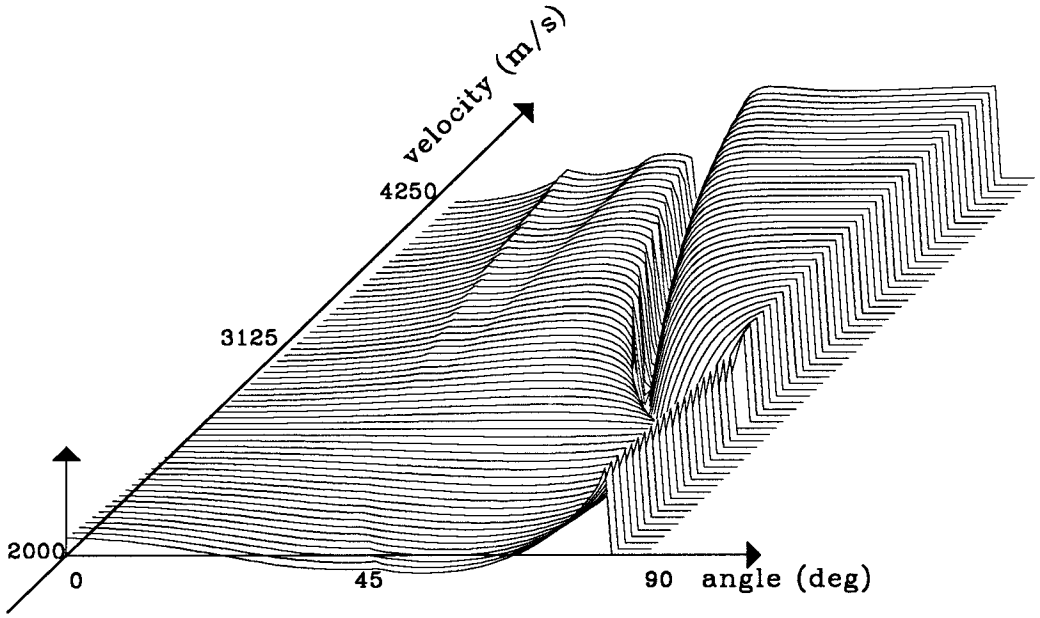

FIG. 8. SS reflection coefficient for the second-third layer interface ($\alpha_2 = 3000$ m/s) as a function of α_3 and the angle of incidence on water.

are not considering in this work the effect of attenuation, which is of fundamental importance for an unconsolidated sea bottom.

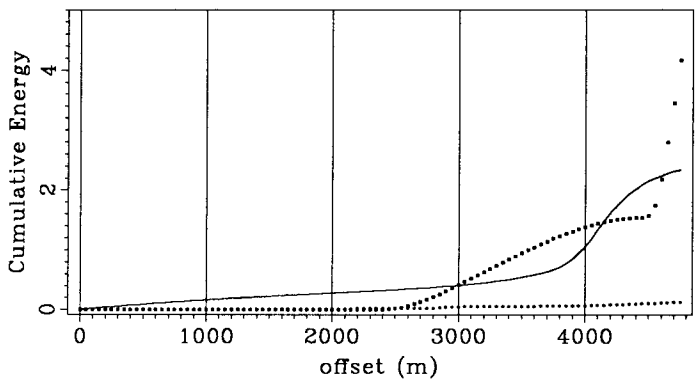

FIG. 9. Cumulative energy X offset for the standard model.

Figure 9 shows the cumulative energy distribution for the standard model. We can see that PSSP has the same overall energy as PPPP for a conventional 3Km's cable, for a large range of second-layer velocities.

A more general picture of the dependence of the energy partition between PPPP and PSSP as a function of the offset is given by Figure 10, which shows how the offset of the intercept point of the cumulative energy changes with respect to the

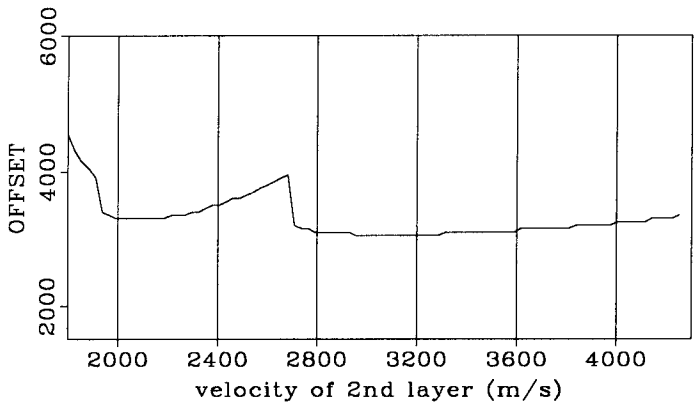

FIG. 10. Intercept point of the cumulative energy for PPPP and PSSP as a function of α_2.

velocity of P waves in the second layer. It is interesting to see that the intercept point for some particular velocities (i.e., 2300 m/s to 2700 m/s) occurs at a larger offset, because of the increase of PP reflection before the critical angle.

CONCLUSIONS

We have found that if the P velocity of the first layer under the water is not very close to the velocity in water, the conventional spreads used on routine seismic surveys will carry a considerable amount of converted mode energy, which will be concentrated on the large offsets. More important is the demonstration that the reflected energy of the PSSP and PPSP/PSPP modes is strongly reduced when gas is present below the reflector. We suggest that the conversion process is worthy of a deeper study, using spherical-waves coefficients and analyzing the applicability of the achieved results on real data.

ACKNOWLEDGMENTS

I would like to thank Francis Muir for the suggestions and discussions that motivated this work. Jon Claerbout and John Etgen also contributed with important suggestions to the final form of this paper.

REFERENCES

Aki, K.I., and Richards, P.G., 1980, Quantitative seismology: W. H. Freeman and Co.

Claerbout, J.F., 1984, Imaging the Earth's Interior: Blackwell Scientific Pub. Inc.

Domenico, S.N., 1984, Rock lithology and porosity determination from shear and compressional wave velocity: Geophysics, **49**, 1188-1195.

Frasier, C.W., 1970, Symmetries in the reflection and transmission of elastic waves: Geophysics, **35**, 197-219.

Ostrander, W.J., 1984, Plane-wave reflection coefficients for gas sands at non normal angles of incidence: Geophysics, **49**, 1637-1648.

Rosa, A. L., 1976, Extraction of elastic parameters using seismic reflection amplitude with offset variations: M.S. thesis, Univ. of Houston.

Tatham, R. H., and Stoffa, P., 1976, V_p V_s - a potential hydrocarbon indicator: Geophysics, **41**, 837-849.

Tatham, R. H., 1982, V_p V_s and lithology : Geophysics, **47**, 336-344.